ATMOSPHERE

Hydrotrioxide (ROOOH) formation in the atmosphere

Torsten Berndt[1]*, Jing Chen[2], Eva R. Kjærgaard[2]†, Kristian H. Møller[2]‡, Andreas Tilgner[1], Erik H. Hoffmann[1], Hartmut Herrmann[1], John D. Crounse[3], Paul O. Wennberg[3,4], Henrik G. Kjaergaard[2]*

Organic hydrotrioxides (ROOOH) are known to be strong oxidants used in organic synthesis. Previously, it has been speculated that they are formed in the atmosphere through the gas-phase reaction of organic peroxy radicals (RO_2) with hydroxyl radicals (OH). Here, we report direct observation of ROOOH formation from several atmospherically relevant RO_2 radicals. Kinetic analysis confirmed rapid RO_2 + OH reactions forming ROOOH, with rate coefficients close to the collision limit. For the OH-initiated degradation of isoprene, global modeling predicts molar hydrotrioxide formation yields of up to 1%, which represents an annual ROOOH formation of about 10 million metric tons. The atmospheric lifetime of ROOOH is estimated to be minutes to hours. Hydrotrioxides represent a previously omitted substance class in the atmosphere, the impact of which needs to be examined.

Hydrotrioxides (ROOOH) are known, thermally unstable products formed in the low-temperature ozonolysis of saturated organic compounds in organic solvents. They are a chemical source of the powerful oxidant singlet molecular oxygen ($^1O_2$) released during their decomposition (*1*, *2*). Accordingly, hydrotrioxides are used in preparative chemistry to form the corresponding oxetane and carbonyl products in the reaction with alkenes mostly carried out at dry-ice temperature (*3*).

In atmospheric gas-phase chemistry, theoretical calculations have proposed the formation of hydrotrioxides as intermediates in the reaction of RO_2 radicals with OH, as shown in pathway 1 below (*4*, *5*). The rapid radical recombination reaction is exothermic by ~130 kJ mol^{-1}, nearly independent of the RO_2 radical, initially forming the energy-rich ROOOH*. This chemically excited species can decompose, leading to the corresponding alkoxy radical RO and HO_2 (pathway 2) or, to a lesser extent, to an alcohol and O_2 (pathway 3). In competition with decomposition, collisions with bath gas molecules, M, result in thermalized ROOOH (pathway 4) (*4*–*6*).

$$RO_2 + OH \rightarrow ROOOH^* \quad (1)$$

$$ROOOH^* \rightarrow RO + HO_2 \quad (2)$$

$$ROOOH^* \rightarrow ROH + O_2 \quad (3)$$

$$ROOOH^* + M \rightarrow ROOOH + M \quad (4)$$

Previous experimental investigations of the RO_2 + OH reaction at 298 K and 50 torr He found a decreasing HO_2 yield, with the RO_2 radical size increasing from C_1 to C_4. For CH_3O_2, the HO_2 yield was 0.90 ± 0.10, which decreased to 0.15 ± 0.03 for n-$C_4H_9O_2$ (*6*). Calculations supported by these experimental findings suggested that at 298 K and 1 bar of N_2, pathway 4 was the dominant fate of ROOOH* in the case of $C_2H_5O_2$ (78%) and larger RO_2 radicals (>95%). For CH_3O_2 radicals, decomposition into CH_3O and HO_2 via pathway 2 still dominates (*6*). Thus, with the exception of CH_3O_2 radicals, formation of the thermalized ROOOH is the expected dominant product from RO_2 + OH reactions in the atmosphere.

There has been a lot of speculation in the literature about the physical chemistry of the reactions of RO_2 radicals with OH in the atmosphere. All evidence that hydrotrioxides are formed has, to date, been indirect, and an experimental proof of hydrotrioxides has been missing up to now (*4*–*7*).

In this work, we conclusively demonstrate, through their direct detection, that hydrotrioxide formation takes place from RO_2 + OH reactions under atmospheric conditions. The investigations were conducted in a free-jet flow system at 295 ± 2 K, a pressure of 1 bar of air, and a reaction time of 7.5 s using product monitoring by chemical ionization mass spectrometry (*8*, *9*). Quantum chemical calculations (*10*–*12*) were carried out in support of the reaction mechanisms as well as the thermal stability and photostability of hydrotrioxides (supplementary materials, section S4).

ROOOH from trimethylamine oxidation

We observed a strong signal consistent with ROOOH formation in the reaction of OH radicals with trimethylamine [$N(CH_3)_3$] using iodide for product ionization in the mass spectrometric detection (fig. S1). In this reaction system, an efficient autoxidation mechanism (*13*) (repeated RO_2 isomerization and O_2 addition) rapidly formed the RO_2 radical $(HOOCH_2)_2NCH_2O_2$ (**I**) as a main product (*10*, *14*). The RO_2 radical (**I**) can react with OH to form the hydrotrioxide (**III**); however, this is in competition with unimolecular RO_2 isomerization forming the dihydroperoxy amide (**II**) and with the RO_2 self-reaction (**I** + **I**) forming the accretion product (**IV**), as illustrated in Fig. 1.

The signal with the mass of the hydrotrioxide $(HOOCH_2)_2NCH_2OOOH$ (**III**) steeply increased with increasing concentrations of the OH precursor, isopropyl nitrite (IPN), i.e., for rising OH and RO_2 radical concentrations in the experiment (Fig. 2A). The signal of **III** behaved similarly to that of the accretion product **IV** formed in the self-reaction of the RO_2 radical **I**. Both followed second-order kinetics, in clear contrast to the first-order kinetics of amide $(HOOCH_2)_2NCHO$ (**II**) formation, arising from the RO_2 isomerization of **I** (*10*). Because OH and RO_2 radical concentrations increased in a similar way with increasing IPN concentrations, the product of the RO_2 + OH reaction increased almost parallel to the accretion product **IV** (Fig. 2A).

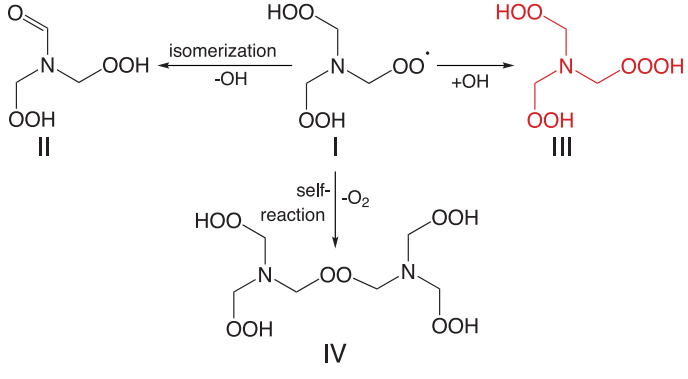

Fig. 1. Product formation starting from the $(HOOCH_2)_2NCH_2O_2$ radical (I).

[1]Atmospheric Chemistry Department (ACD), Leibniz Institute for Tropospheric Research (TROPOS), 04318 Leipzig, Germany. [2]Department of Chemistry, University of Copenhagen, DK-2100 Copenhagen Ø, Denmark. [3]Division of Geological and Planetary Sciences, California Institute of Technology, Pasadena, CA 91125, USA. [4]Division of Engineering and Applied Science, California Institute of Technology, Pasadena, CA 91125, USA.
*Corresponding author. Email: berndt@tropos.de (T.B.); hgk@chem.ku.dk (H.G.K.)
†Present address: Department of Chemistry, Aarhus University, DK-8000 Aarhus C, Denmark.
‡Present address: Niels Bohr Institute, University of Copenhagen, DK-1350 Copenhagen, Denmark.

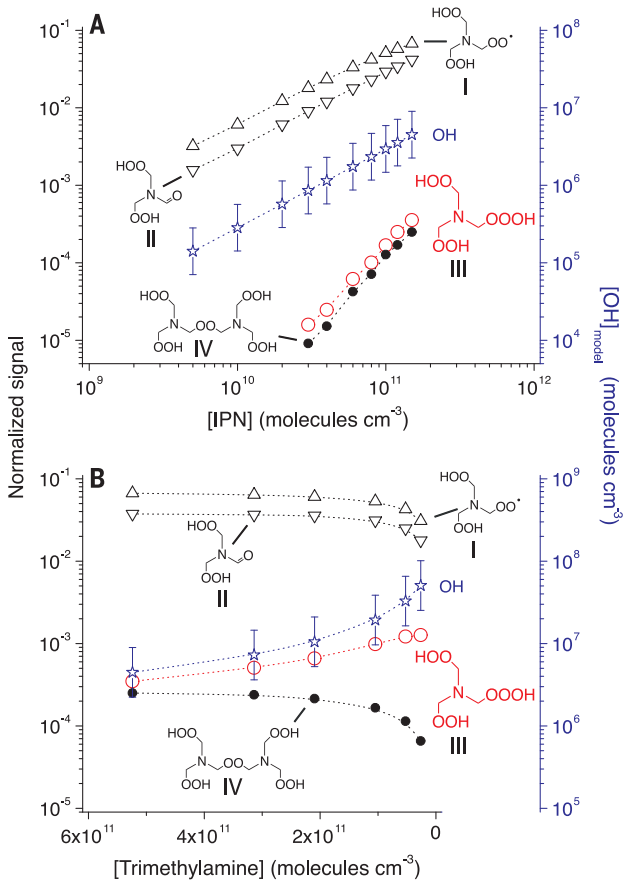

Fig. 2. Product formation from OH + trimethylamine for increasing OH levels. (**A**) Rising OH and RO_2 radical levels were the result of increasing IPN for otherwise constant reactant concentrations, [NO] = 1.0 × 10^{10} and [trimethylamine] = 5.2 × 10^{11} molecules cm^{-3}. (**B**) Rising OH levels resulted from constant OH production, i.e., constant IPN and NO concentrations ([IPN] = 1.5 × 10^{11} and [NO] = 1.0 × 10^{10} molecules cm^{-3}), and lowering of the main OH consumer trimethylamine. In both experiments, OH radicals were produced from IPN photolysis in air whereby the OH generation finally proceeded via NO + HO_2 → OH + NO_2. Product signals were measured with a standard deviation of <20%. Stated OH concentrations were taken from modeling with an assumed uncertainty of a factor of 2.

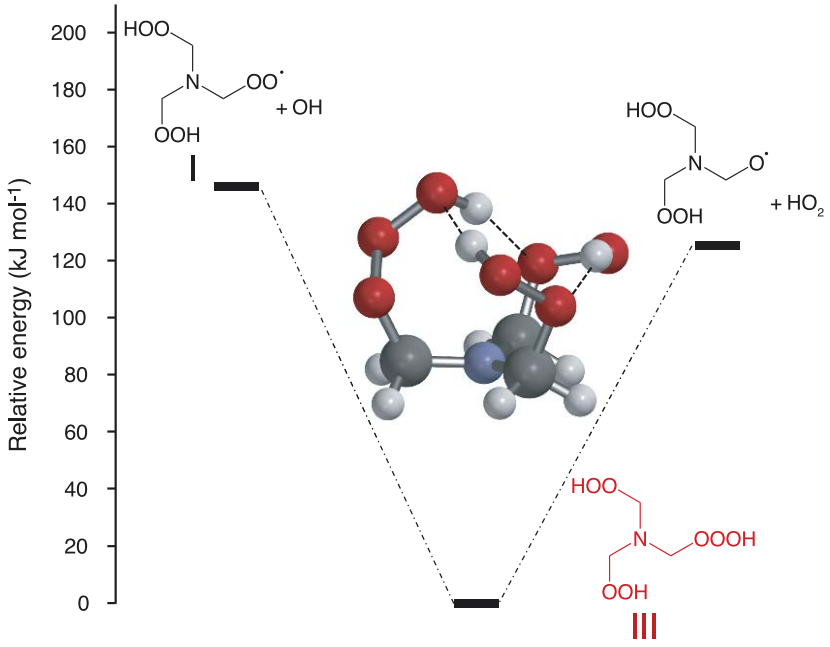

Fig. 3. Energy diagram for the formation of hydrotrioxide $(HOOCH_2)_2NCH_2OOOH$ (III). Its formation from $(HOOCH_2)_2NCH_2OO$ (**I**) + OH was exothermic by 146 kJ mol^{-1}, and its decomposition into the corresponding alkoxy radical + HO_2 was endothermic by 126 kJ mol^{-1}. The lowest-energy conformer of the hydrotrioxide is shown, and dashed lines illustrate the three hydrogen bonds. The zero-point vibrational energy–corrected electronic energies were calculated at the UCCSD(T)-F12a/cc-pVDZ-F12//M06-2X/aug-cc-pVTZ level.

For further mechanistic validation of ROOOH formation, we increased the OH level in the experiment by lowering the trimethylamine concentration for a constant OH production rate using unchanged IPN and nitric oxide (NO) in the photolysis (Fig. 2B). The OH level grew as a result of the decreasing OH loss rate with the lowering of the main OH consumer trimethylamine. At sufficiently small trimethylamine concentrations, OH started to react substantially with CO, methane, and other trace gases in the air, resulting in clear weakening of the RO_2 radical **I** production (Fig. 2B). Simultaneously, the signals of the RO_2 isomerization product **II** and the accretion product **IV** declined. By contrast, the signal attributed to the hydrotrioxide **III** showed a clear increase with increasing OH levels, which emphasizes that **III** has to be formed in a second OH reaction subsequent to the initial OH + trimethylamine reaction that forms **I**. Additional tests revealed that the hydrotrioxide formation was not influenced by interfering processes during product ionization and photolysis (fig. S2), or by the presence of water vapor (fig. S3), or by elevated NO concentrations (fig. S4). Using modeled OH concentrations (supplementary materials, section S1.5), we found a linear dependence of signal(ROOOH) versus signal(RO_2) × $[OH]_{model}$ in accord with the expected formation mechanism of ROOOH (fig. S5). OH radical measurements in amine systems were not possible with our technique.

The same product formation from OH + trimethylamine, including hydrotrioxide production, was also measured using nitrate as the reagent ion (fig. S6). H/D exchange experiments in the presence of heavy water (*8*, *15*) (to determine the number of weakly bound, exchangeable H atoms) showed a signal shift by 3 mass units in the mass spectrum, in accord with the presence of two OOH groups and the OOOH group further supporting the structure of **III** (fig. S7). All experimental findings were consistent with the formation of the hydrotrioxide **III** through a RO_2 + OH reaction.

In Fig. 3, we show the calculated energy diagram of reactions 1 and 2 for the observed hydrotrioxide $(HOOCH_2)_2NCH_2OOOH$. The decomposition of the hydrotrioxide leading to the alkoxy radical and HO_2 was ~20 kJ mol^{-1} lower in energy than that leading to the RO_2 radical and OH, which is in overall agreement with previous calculations performed on small C_1 to C_4 hydrotrioxides (*4*, *6*). Formation of three strong internal hydrogen bonds in $(HOOCH_2)_2NCH_2OOOH$ increased its thermostability compared with that of less-functionalized hydrotrioxides (supplementary materials, section S4.2).

ROOOH from isoprene oxidation

ROOOH formation was also probed in the reaction of OH radicals with isoprene (C_5H_8), one

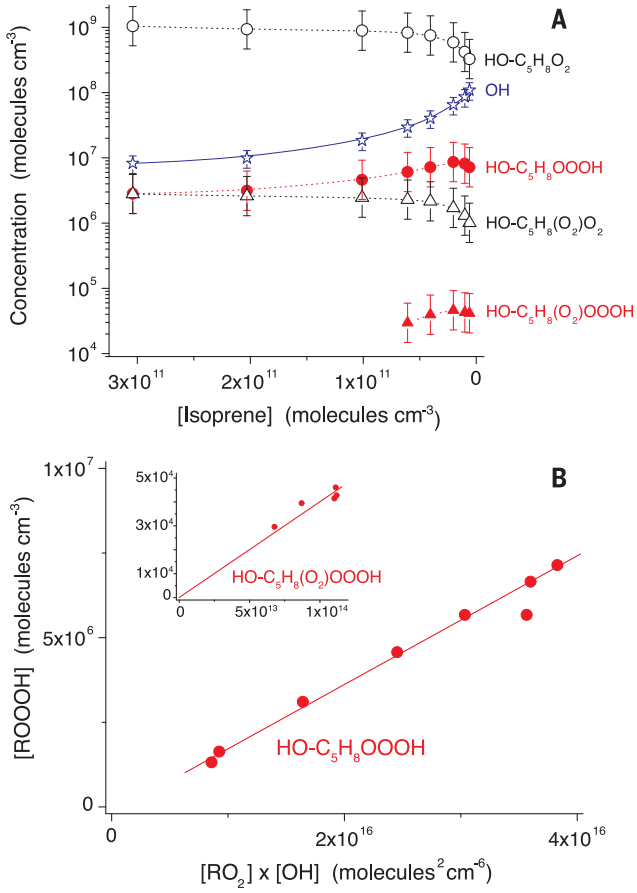

Fig. 4. Product formation and ROOOH formation kinetics in the OH + isoprene reaction. (**A**) Product concentrations were obtained using calibration factors from former investigations (supplementary materials, section S1.3). Corresponding error bars have been determined from the uncertainty in the calibration factors. OH concentrations were derived from detection of SO_3 formed via OH + SO_2. Increasing OH concentrations (blue stars) for constant OH production in the IPN photolysis ([IPN] = 2.15 × 10^{11} and [NO] = 1.0 × 10^{10} molecules cm^{-3}) were the result of lowering of the OH loss rate by reducing the main consumer isoprene. Iodide was used as the reagent ion. The uncertainty of OH concentrations has been estimated to be ~30% considering the uncertainties of the SO_3 calibration and in k(OH + SO_2). (**B**) Data were taken from the experiments depicted in (A). Deduced rate coefficients of HO-C_5H_8OOOH and HO-$C_5H_8(O_2)OOOH$ formation from RO_2 + OH were 5.1 × 10^{-11} and 1.1 × 10^{-10} cm^3 $molecule^{-1}$ s^{-1}, respectively. Error bars are not shown for clarity.

of the most important nonmethane hydrocarbons in the atmosphere (fig. S8) (*16*). In this case, different isomeric RO_2 radicals were formed as a result of isoprene's structure and the different positions of OH and O_2 addition as well as the RO_2 interconversion in this system (*17*, *18*). Moreover, RO_2 autoxidation led to a suite of different oxidized RO_2 radicals HO-$C_5H_8(O_2)_xO_2$, where x = 0, 1, and 2 (*9*, *12*, *17*–*19*). In Fig. 4A, we show the results from an experiment with rising OH level resulting from the lowering of isoprene in the reaction gas for constant photolysis conditions. The OH concentration was determined indirectly by monitoring SO_3 formation from OH + SO_2. The small SO_2 addition did not disturb the OH + isoprene reaction (fig. S9). Signals consistent with hydrotrioxides HO-$C_5H_8(O_2)_xOOOH$, where x = 0 and 1, emerged beside those from the corresponding RO_2 radicals. Both substance classes showed the expected behavior, i.e., the RO_2 radical concentrations decreased with the lowering of the isoprene concentration, and the ROOOH compounds increased proportional to the product [RO_2] × [OH]. Experiments with rising OH and RO_2 radical concentrations, as a result of increasing IPN concentrations, confirmed these findings (fig. S10).

The ROOOH formation kinetics were assessed on the basis of the measured ROOOH, RO_2, and OH radical concentrations (Fig. 4B). From the linear dependence of [ROOOH] versus [RO_2] × [OH] in the case of HO-C_5H_8OOOH, a rate coefficient of k(HO-$C_5H_8O_2$ + OH) = 5.1 × 10^{-11} cm^3 $molecule^{-1}$ s^{-1} follows. For the higher oxidized HO-$C_5H_8(O_2)OOOH$, the analysis yields k(HO-$C_5H_8(O_2)O_2$ + OH) = 1.1 × 10^{-10} cm^3 $molecule^{-1}$ s^{-1}, assuming a regression line through zero (Fig. 4B, inset). These rate coefficients have an uncertainty of a factor of 3 to 4. Previously, high rate coefficients of RO_2 + OH reactions were reported for C_1 to C_4 RO_2 radicals through detection of the OH decay, e.g., k($C_4H_9O_2$ + OH) = (1.5 ± 0.3) × 10^{-10} cm^3 $molecule^{-1}$ s^{-1} at 298 K (*20*), which supports our findings.

Universal ROOOH formation

We tested the general validity of hydrotrioxide formation from RO_2 + OH reactions, especially for RO_2 radicals with atmospheric relevance. In the OH radical–initiated oxidation of dimethyl sulfide (DMS), α-pinene, toluene, and 1-butene, the corresponding hydrotrioxide formation from the principal RO_2 radicals in the respective reaction system was clearly detectable in the flow experiment (figs. S11 to S18). Data analysis revealed a linear dependence of signal(ROOOH) versus signal(RO_2) × [OH] for each system (figs. S19 to S22). In the cases where RO_2 radicals and ROOOH could be detected with close-to-maximum sensitivity, the rate coefficients k(RO_2 + OH) were estimated (figs. S5 and S20), further supporting that RO_2 + OH reactions proceed with rate coefficients close to the collision limit. Table S2 summarizes the rate coefficients determined in this study. Moreover, signals consistent with hydrotrioxide formation from the reaction of OH radicals with 2-methylpropene were observed in separate experiments conducted in a 1-m^3 Teflon (fluorinated ethylene propylene) chamber in air using CF_3O^- chemical ionization mass spectrometry (supplementary materials, section S1.7, and fig. S23). Consequently, it could be inferred that RO_2 + OH reactions represent a universal pathway of hydrotrioxide formation under atmospheric conditions.

Atmospheric perspective of ROOOH

The hydroxy hydrotrioxide formed in the OH + 2-methylpropene reaction, as observed in the environmental chamber experiment (fig. S23), suggested an experimental ROOOH lifetime of ~20 min at 296 K including thermal gas-phase decomposition and losses on the chamber wall. Thus, 20 min can be regarded as a lower bound of its thermal lifetime. Theoretical calculations on the thermal decomposition energies (Fig. 3) for several hydrotrioxides pointed to similar or longer thermal lifetimes (supplementary materials, section S4.2). In addition, the calculations did not indicate any fast photolysis pathways for ROOOH (supplementary materials, section S4.3).

We estimated the atmospheric lifetime of hydrotrioxides against the OH reaction to be ~2 hours to a few days assuming [OH] = (5 to 20) × 10^5 molecules cm^{-3} and k(OH + ROOOH) = (1 to 7.5) × 10^{-11} cm^3 $molecule^{-1}$ s^{-1}, relevant for saturated and unsaturated hydrotrioxides assuming an OH reactivity similar to that of the corresponding hydroperoxides (*21*, *22*). Thus, hydrotrioxides, once formed, would be present in the atmosphere for minutes to hours before further processing. Theoretical calculations favored the formation of alkoxy radicals RO from the reaction of OH radicals with saturated ROOOH. In the isoprene system, however, OH + HO-C_5H_8OOOH mainly forms the dihydroxy epoxide IEPOX (*18*) and HO_2 (supplementary materials, section S4.5).

Global simulations with the chemistry climate model ECHAM-HAMMOZ (*23*) permitted an assessment of ROOOH production from

the OH radical–initiated oxidation of isoprene (figs. S24 and S25). We lumped all isoprene-derived RO_2 radicals and calculated that up to 1% of these could react with OH, forming ROOOH. Given the large emission of isoprene (*16*), an annual ROOOH production of up to ~10 million metric tons is calculated. Furthermore, the modeling revealed that isoprene-derived hydrotrioxides can reach atmospheric concentrations of ~10^7 molecules cm^{-3} (fig. S24).

From the knowledge in preparative chemistry (*1*–*3*), we deduced that hydrotrioxides could act as oxidants. In the atmosphere, this reactivity could manifest itself in surface reactions after lung inhalation and reactions on and within aerosol particles forming $^1O_2$. Hydrotrioxides generated from highly oxidized RO_2 radicals represent highly oxygenated organic molecules (HOMs) (*24*) with a very large oxygen content, e.g., HO-$C_{10}H_{16}(O_2)_2OOOH$ (fig. S14). These ROOOH-HOMs would be relevant for atmospheric aerosol formation and thus for Earth's radiation budget. Further research is needed to ascertain the role of hydrotrioxides for health and the environment. We illustrated the direct observation of hydrotrioxides using mass spectrometry, which should open up opportunities to measure these compounds in different systems, including in the atmosphere, after further optimization of the analytical techniques.

REFERENCES AND NOTES

1. F. E. Stary, D. E. Emge, R. W. Murray, *J. Am. Chem. Soc.* **98**, 1880–1884 (1976).
2. M. Zarth, A. De Meijere, *Chem. Ber.* **118**, 2429–2449 (1985).
3. G. H. Posner, K. S. Webb, W. M. Nelson, T. Kishimoto, H. H. Seliger, *J. Org. Chem.* **54**, 3252–3254 (1989).
4. J. F. Müller *et al*., *Nat. Commun.* **7**, 13213 (2016).
5. Y. Liu *et al*., *Chem. Res. Chin. Univ.* **33**, 623–630 (2017).
6. E. Assaf, C. Schoemaecker, L. Vereecken, C. Fittschen, *Int. J. Chem. Kinet.* **50**, 670–680 (2018).
7. A. T. Archibald, A. S. Petit, C. J. Percival, J. N. Harvey, D. E. Shallcross, *Atmos. Sci. Lett.* **10**, 102–108 (2009).
8. T. Berndt *et al*., *Nat. Commun.* **7**, 13677 (2016).
9. T. Berndt, N. Hyttinen, H. Herrmann, A. Hansel, *Commun. Chem.* **2**, 21 (2019).
10. K. H. Møller, T. Berndt, H. G. Kjaergaard, *Environ. Sci. Technol.* **54**, 11087–11099 (2020).
11. E. Praske *et al*., *Proc. Natl. Acad. Sci. U.S.A.* **115**, 64–69 (2018).
12. K. H. Møller, K. H. Bates, H. G. Kjaergaard, *J. Phys. Chem. A* **123**, 920–932 (2019).
13. J. D. Crounse, L. B. Nielsen, S. Jørgensen, H. G. Kjaergaard, P. O. Wennberg, *J. Phys. Chem. Lett.* **4**, 3513–3520 (2013).
14. T. Berndt, K. H. Møller, H. Herrmann, H. G. Kjaergaard, *J. Phys. Chem. A* **125**, 4454–4466 (2021).
15. M. P. Rissanen *et al*., *J. Am. Chem. Soc.* **136**, 15596–15606 (2014).
16. K. Sindelarova *et al*., *Atmos. Chem. Phys.* **14**, 9317–9341 (2014).
17. J. Peeters, T. L. Nguyen, L. Vereecken, *Phys. Chem. Chem. Phys.* **11**, 5935–5939 (2009).
18. P. O. Wennberg *et al*., *Chem. Rev.* **118**, 3337–3390 (2018).
19. S. Wang, M. Riva, C. Yan, M. Ehn, L. Wang, *Environ. Sci. Technol.* **52**, 12255–12264 (2018).
20. E. Assaf, S. Tanaka, Y. Kajii, C. Schoemaecker, C. Fittschen, *Chem. Phys. Lett.* **684**, 245–249 (2017).
21. J. M. St. Clair *et al*., *J. Phys. Chem. A* **120**, 1441–1451 (2016).
22. C. Fittschen *et al*., *Atmos. Chem. Phys.* **19**, 349–362 (2019).
23. M. G. Schultz *et al*., *Geosci. Model Dev.* **11**, 1695–1723 (2018).
24. F. Bianchi *et al*., *Chem. Rev.* **119**, 3472–3509 (2019).
25. J. Chen, K. H. Møller, E. R. Kjaergaard, H. G. Kjaergaard, ROOOH-archive, Electronic Research Data Archive (University of Copenhagen, 2022); https://doi.org/10.17894/UCPH.99BF9F39-EC48-4AFE-B426-CF6EF0D3EA70.
26. E. H. Hoffmann, A. Tilgner, H. Herrmann, ROOOH modeling data — archive, Zenodo (2022); https://doi.org/10.5281/zenodo.6373045.

ACKNOWLEDGMENTS

The authors thank A. Rohmer and K. Pielok for technical assistance and the tofTools team for providing the data analysis tools. This work used resources of the Deutsches Klimarechenzentrum (DKRZ) granted by its Scientific Steering Committee (WLA) under project ID bb1128. **Funding:** H.G.K. acknowledges funding from the Independent Research Fund Denmark (9040-00142B) and the High Performance Computing Center at the University of Copenhagen. E.H.H. and H.H. acknowledge funding from the German Research Foundation (project ORIGAMY, no. 447349939). P.O.W. and J.D.C. received financial support from the US National Science Fund (CHE-1905340). P.O.W. and H.G.K. received funding from the Alfred P. Sloan Foundation under award no. G-2019-12281. **Author contributions:** Conceptualization: T.B. and H.G.K. Methodology: All authors. Experiments: T.B. and J.D.C. Calculations: J.C., E.R.K., K.H.M., and H.G.K. Global modeling: A.T., E.H.H., H.H., and P.O.W. Writing – original draft: T.B. and H.G.K. Writing – review and editing: All authors. **Competing interests:** The authors declare that they have no competing interests. **Data and materials availability:** All theoretical calculation output files are available online through the public research data archive of the University of Copenhagen (*25*). All ECHAM-HAMMOZ model output files are available online through the public research data archive Zenodo (*26*). All other data are available in the main text or the supplementary materials.

SUPPLEMENTARY MATERIALS

science.org/doi/10.1126/science.abn6012
Materials and Methods
Figs. S1 to S47
Tables S1 to S10
References (*27*–*67*)

Submitted 8 December 2021; accepted 20 April 2022
10.1126/science.abn6012

Hydrotrioxide (ROOOH) formation in the atmosphere

Torsten BerndtJing ChenEva R. KjærgaardKristian H. MøllerAndreas TilgnerErik H. HoffmannHartmut HerrmannJohn D. CrounsePaul O. WennbergHenrik G. Kjaergaard

Science, 376 (6596), • DOI: 10.1126/science.abn6012

Powerful oxidants in the atmosphere

Hydrotrioxides (ROOOHs) have intrigued the atmospheric chemistry community because of their strong oxidizing properties and theoretical predictions that they could form in atmospherically relevant RO + OH reactions. Much of the work to date has focused on CHO, but this chemistry has been found to play a minor role. Using a mass spectrometry–based scheme for direct detection and ab initio calculations supplemented by global modeling, Berndt *et al*. showed that ROOOHs could form routinely for heavier RO and have appreciable lifetimes. Potentially detectable steady-state concentrations in the atmosphere were established. This work draws attention to an important class of strong oxidizing agents previously disregarded in atmospheric kinetics models. —YS